Journal of Structural Engineering Vol.49A(March 2003) JSCE

AN EXTENDED ELASTIC SHEAR DEFORMABLE BEAM THEORY AND ITS APPLICATION TO CORRUGATED STEEL WEB GIRDER

Chawalit MACHIMDAMRONG*, Eiichi WATANABE** and Tomoaki UTSUNOMIYA***

*Student member of JSCE, Graduate Student, Dept. of Civil Eng., Kyoto University
Yoshida-honmachi, Sakyo-ku, Kyoto 606-8501, Japan
**Fellow of JSCE, Ph. D., Dr. Eng., Professor, Dept. of Civil Eng., Kyoto University
Yoshida-honmachi, Sakyo-ku, Kyoto 606-8501, Japan
***Member of JSCE, Dr. Eng., Associate Professor, Dept. of Civil Eng., Kyoto University
Yoshida-honmachi, Sakyo-ku, Kyoto 606-8501, Japan

Composite PC girder with corrugated steel web is a promising alternative of new bridge construction nowadays. A number of advantage over conventional flat straight web PC bridge are owing to its marked separation of functions in resisting shearing force by corrugated web and bending force by upper and lower flanges. However, considerable shear deformation in the web causes the deformed section of concrete flanges and that of the web unparalleled. This results in errors when the Euler–Bernoulli beam theory is applied for stress and deflection analysis of the girder. In this study, a more refined beam theory which accounts for shear deformation is derived by the variational principle. Equilibrium equations and boundary conditions for the theory based on three and two independent displacement functions are obtained. The general solution of the differential equations are presented and applied to predict shearing force and deflection in a number of girder comparing to results calculated by the finite element analysis. A good agreement on the results is found and it is concluded that the theory is applicable to be used for predicting force and deflection in the composite PC girder with corrugated steel web.

Key Words: Extended beam theory, Shear deformable beam, Variational principle, Corrugated steel web, Finite element analysis.

1. Introduction

It is well known that folding a flat metal sheet to a corrugated plate can increase flexural stiffness in a direction parallel to its folded edges and it has been used for many years in shipbuilding, for containers and for long span roof beams [1)].

The increase in flexural stiffness and its other advantages were also noticed from bridge construction side and it was applied successfully in construction of the first PC bridge utilizing the corrugated steel plate as its web in France [2)]. The successfulness and its remarkable advantages over conventional PC bridge has aroused a number of research activity and construction company to get involving in this new hybrid structure, especially in Japan.

More than ten PC box girder bridges with corrugated steel web were constructed and under construction in Japan with a maximum clear span already exceeding 130 m [3)]. An effort to put the PC bridge with corrugated steel web into concrete practice in Japan is evident on a publication of the design manual by Research Group of Composite Structures with Corrugated Steel Web in 1998 [4)].

On the academic side, PC bridge with corrugated steel web and its relevant subjects have attracted a number of research activities worldwide. Lot of research papers on the subjects are found originated from U.S., Japan, European countries and Taiwan [5) 6)].

The most prominent advantages of the PC box girder bridge with corrugated steel web are [3) 7)]: 1) Reduction in the weight of web and therefore the weight of the bridge. 2) Prestressing can be efficiently introduced due to the so-called "accordion effect" of the corrugated web [8)]. 3) No need for additional stiffeners for web because of its high shear buckling strength. 4) Easiness for the long-term repair and maintenance. Other advantages not argued here can be found in a paper by Johnson and Cafolla [5)].

The corrugated steel web in a PC girder functions mainly as a vertical shear–resisting member, while upper and lower concrete flanges resist for bending moment. A number of researches have been carried out to investigate this characteristic and can be found, for example in an experiment work of Yamaguchi *et al.* [8)] and those of Elgaaly *et al.* [9) 10)].

Separation of the function of the girder in this way may retard transfer of shear force to the corrugated web, especially near a point of applied loading. This phenomenon is called shear lag and is known to occur peculiarly in thin-walled structures. The retarding of shear transfer is also found in partially interactive composite beam, however with different cause [11].

The dominant shear deformation in the corrugated web of the composite girder causes deformed section of the flanges and that of the web unparalleled (see Figure 1). This phenomenon gives rise to an error in applying the Euler–Bernoulli beam theory to study stress state and deformation of the girder.

To understand the phenomenon, a simple numerical method based on a laminated beam theory was given by Taniguchi and Yoda [12]. Nonlinear analysis and comparison to experimental results were also included in their work.

Shirozu *et al.* [13] attacked the problem by another numerical method based on the so–called "Constant shear flow panels". The girder is divided into a number of small section and the assumption on constant shear flow is postulated on each panel. This method has an advantage when the girder is of varied depth because of its sectioning scheme.

Later on, an analytical treatment is provided in a work of Kato *et al.* [14]. The corrugated web is assumed to be capable to carry only shearing force with negligible bending capacity. Two independent functions are introduced in the formulation. The equilibrium equations are derived based on force equilibrium on a section. However, underestimation of shearing force in the flanges is observed.

In this study, a more precise beam theory based on shear deformable Timoshenko beam hypothesis is presented. Three–function beam theory based on beam's vertical displacement, rotation of web and identical rotation of upper and lower flanges is derived by the variational principle. The approach is justified because the correct form of differential equations and boundary conditions for assumed displacement field are not known without using the virtual work principles [15]. A reduction to two–function beam theory is also carried out. This theory is similar but not identical to that derived by Kato *et al.* [14].

The derived differential equations are then solved for homogeneous solution and a particular solution for a case of uniformly distributed transverse load. Application of the theories to predict shearing force and deflection in a number of girders is carried out and compared with those calculated by the finite element method.

2. Theoretical development

Theoretical development is based on two–dimensional treatment in plane of longitudinal direction along girder axis (x-axis) and in vertical direction along depth of the beam (z-axis), see Figure 1. Concrete and steel materials are assumed isotropic and homogeneous and they are free from initial strain and residual stress. All element on a line perpendicular to x-z plane is assumed to have the same stress and strain state (Plane stress condition). Poisson's ratios are assumed to be zero in all material.

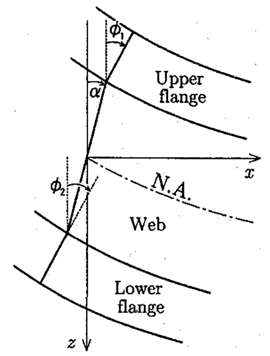

Figure 1: Typical sectional deformation of PC girder with corrugated web and assumed rotations

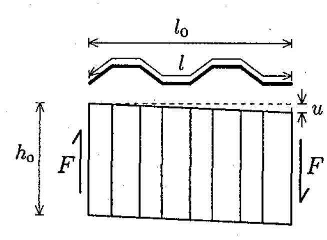

Figure 2: Shear deformation of corrugated web

However, it is used to calculate shear modulus of elasticity. Normal stress in z-direction is negligible because it is small compared with normal stresses in x-direction [16]. These are the common assumptions in general derivation of an in–plane behavior of beam theory.

It is required further that, the connection between concrete flanges and steel web is assumed perfect. All stresses are within elastic region and there is no crack in concrete flanges (it is actually restricted by prestressing force which is not considered here)

The corrugated web is considered to be a flat plate with equivalent thickness, t_0 with reduced modulus of elasticity, E_0. The transform equation for the equivalent thickness can be derived by considering that the corrugated web is continuously attached to "semi–rigid" diaphragms, i.e., diaphragms that preserve the shape of the end cross sections but offer no resistance to the warping of these cross sections out of their planar condition [4] [17]. Shearing force in the web can then be expressed as shown below (Figure 2):

$$F = G_0 A \gamma = G_0 (h_0 t) \left(\frac{u}{l}\right) = G_0 h_0 \left(\frac{l_0}{l} t\right) \frac{u}{l_0}. \quad (1)$$

Here, G_0 is shear modulus of elasticity of the web and t is its actual thickness. The equivalent thickness of the corrugated web can now be written as:

$$t_0 = \frac{l_0}{l} t. \quad (2)$$

The assumed displacements for the girder are as

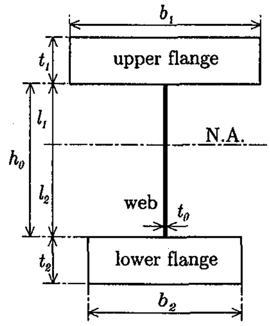

Figure 3: Cross sectional dimensions of the girder

shown below (see Figure 1):

$$\begin{aligned} u^{\mathcal{W}}(x,z) &= -z\ \alpha(x), \\ u^{\mathcal{U}}(x,z) &= l_1\ \alpha(x) - (z+l_1)\ \phi_1(x), \\ u^{\mathcal{L}}(x,z) &= -l_2\ \alpha(x) - (z-l_2)\ \phi_2(x), \\ w^{\mathcal{W}}(x) &= w^{\mathcal{U}}(x) = w^{\mathcal{L}}(x) = w(x). \end{aligned} \tag{3}$$

Superscript $\mathcal{W}$, $\mathcal{U}$ and $\mathcal{L}$ refer to web, upper flange and lower flange, respectively. Geometric dimensions, l_1, l_2, etc. are shown schematically in Figure 3. There are four unknown functions in the above assumption namely vertical deflection of the girder (w), rotation of the upper flange (ϕ_1), rotation of the lower flange (ϕ_2) and rotation of the web (α). The assumption is generous, however, complexity arises with this assumption in determining a location of the neutral axis.

The neutral axis of a given section is defined as a point (or a line perpendicular to x-z plane) on the section with no longitudinal strain and it can be found by equilibrium of horizontal force on the section:

$$\begin{aligned} 0 &= \int_A \sigma_{xx}\,\mathrm{d}A. \\ 0 &= b_1 E_1 \int_{-l_1-t_1}^{-l_1} \frac{\partial u^{\mathcal{U}}}{\partial x}\,\mathrm{d}z + t_0 E_0 \int_{-l_1}^{l_2} \frac{\partial u^{\mathcal{W}}}{\partial x}\,\mathrm{d}z \\ &\quad + b_2 E_2 \int_{l_2}^{l_2+t_2} \frac{\partial u^{\mathcal{L}}}{\partial x}\,\mathrm{d}z. \end{aligned} \tag{4}$$

Modulus of elasticity for upper flange and lower flange are designated as E_1 and E_2, respectively.

Substituting the assumed displacements (Equation 3) into Equation 4 and note that $l_2 = h_0 - l_1$, $A_0 = t_0 h_0$, $A_1 = b_1 t_1$ and $A_2 = b_2 t_2$, one can write an expression for l_1 as:

$$l_1 = \frac{h_0\,(E_0A_0 + 2E_2A_2)\,\frac{\mathrm{d}\alpha}{\mathrm{d}x} - E_1A_1t_1\frac{\mathrm{d}\phi_1}{\mathrm{d}x} + E_2A_2t_2\frac{\mathrm{d}\phi_2}{\mathrm{d}x}}{2\,(E_0A_0 + E_1A_1 + E_2A_2)\,\frac{\mathrm{d}\alpha}{\mathrm{d}x}}. \tag{5}$$

It is evident that the location of neutral axis depends on three functions and this complicates later development by its non-linearity. However, it is thought that at a section far from a point of abrupt change in shearing force, the neutral axis is nearly equal to that calculated simply by first-moment method. From this fact and to allow further development, the location of neutral axis is assumed constant along the girder and equal to that calculated by first-moment equation.

2.1 Three–Function Beam Theory

In general, dimensions of cross section of upper and lower flanges are in the same order (comparing to the web), identical rotation in upper flange and lower flange is then assumed, $\phi_2 = \phi_1 = \phi$. The assumed displacement functions and their normal and shear strains can be written as shown below:

$$\begin{aligned} u^{\mathcal{W}} &= -z\,\alpha, \\ u^{\mathcal{U}} &= l_1\,\alpha - (z+l_1)\,\phi, \\ u^{\mathcal{L}} &= -l_2\,\alpha - (z-l_2)\,\phi, \\ w^{\mathcal{W}} &= w^{\mathcal{U}} = w^{\mathcal{L}} = w. \end{aligned} \tag{6}$$

$$\begin{aligned} \varepsilon^{\mathcal{W}}_{xx} &= -z\frac{\mathrm{d}\alpha}{\mathrm{d}x}, & \gamma^{\mathcal{W}}_{xz} &= \frac{\mathrm{d}w}{\mathrm{d}x} - \alpha, \\ \varepsilon^{\mathcal{U}}_{xx} &= l_1\frac{\mathrm{d}\alpha}{\mathrm{d}x} - (z+l_1)\frac{\mathrm{d}\phi}{\mathrm{d}x}, & \gamma^{\mathcal{U}}_{xz} &= \frac{\mathrm{d}w}{\mathrm{d}x} - \phi, \\ \varepsilon^{\mathcal{L}}_{xx} &= -l_2\frac{\mathrm{d}\alpha}{\mathrm{d}x} - (z-l_2)\frac{\mathrm{d}\phi}{\mathrm{d}x}, & \gamma^{\mathcal{L}}_{xz} &= \frac{\mathrm{d}w}{\mathrm{d}x} - \phi. \end{aligned} \tag{7}$$

All shear strains in Equation 7 are the same as defined in the Timoshenko beam theory [18) 19)]. By the fact that shear strain in the web ($\gamma^{\mathcal{W}}_{xz}$) is almost constant along its vertical panel, there is no requirement on a shear correction factor for this element. However, for the upper and lower flanges, a shear correction factor of 5/6 is used to compensate for free surface stress condition in Timoshenko beam theory.

In this study, the variational principle [20)] is used to formulate the equations of equilibrium and the boundary condition of the system. The required energy functions in the principle are derived and presented below.

The virtual strain energy of the beam along beam span ($0 \leqslant x \leqslant L$), can be written as:

$$\begin{aligned} \delta U &= \int_0^L \int_A (\sigma_{xx}\delta\varepsilon_{xx} + \tau_{xz}\delta\gamma_{xz})\,\mathrm{d}A\,\mathrm{d}x \\ &= \delta U^{\mathcal{W}} + \delta U^{\mathcal{U}} + \delta U^{\mathcal{L}}, \end{aligned} \tag{8}$$

$$\begin{aligned} \delta U^{\mathcal{W}} &= t_0 \int_0^L \int_{-l_1}^{l_2} (\sigma^{\mathcal{W}}_{xx}\delta\varepsilon^{\mathcal{W}}_{xx} + \tau^{\mathcal{W}}_{xz}\delta\gamma^{\mathcal{W}}_{xz})\,\mathrm{d}z\,\mathrm{d}x \\ &= \int_0^L \left\{ -M^{\mathcal{W}}\frac{\mathrm{d}\delta\alpha}{\mathrm{d}x} + Q^{\mathcal{W}}\left(\frac{\mathrm{d}\delta w}{\mathrm{d}x} - \delta\alpha\right) \right\}\mathrm{d}x, \\ \delta U^{\mathcal{U}} &= b_1 \int_0^L \int_{-(l_1+t_1)}^{-l_1} (\sigma^{\mathcal{U}}_{xx}\delta\varepsilon^{\mathcal{U}}_{xx} + \tau^{\mathcal{U}}_{xz}\delta\gamma^{\mathcal{U}}_{xz})\,\mathrm{d}z\,\mathrm{d}x \\ &= \int_0^L \left\{ N^{\mathcal{U}} l_1 \frac{\mathrm{d}\delta\alpha}{\mathrm{d}x} - (M^{\mathcal{U}} + N^{\mathcal{U}} l_1)\frac{\mathrm{d}\delta\phi}{\mathrm{d}x} \right. \\ &\qquad \left. + Q^{\mathcal{U}}\left(\frac{\mathrm{d}\delta w}{\mathrm{d}x} - \delta\phi\right) \right\}\mathrm{d}x, \\ \delta U^{\mathcal{L}} &= b_2 \int_0^L \int_{l_2}^{l_2+t_2} (\sigma^{\mathcal{L}}_{xx}\delta\varepsilon^{\mathcal{L}}_{xx} + \tau^{\mathcal{L}}_{xz}\delta\gamma^{\mathcal{L}}_{xz})\,\mathrm{d}z\,\mathrm{d}x \\ &= \int_0^L \left\{ -N^{\mathcal{L}} l_2 \frac{\mathrm{d}\delta\alpha}{\mathrm{d}x} - (M^{\mathcal{L}} - N^{\mathcal{L}} l_2)\frac{\mathrm{d}\delta\phi}{\mathrm{d}x} \right. \\ &\qquad \left. + Q^{\mathcal{L}}\left(\frac{\mathrm{d}\delta w}{\mathrm{d}x} - \delta\phi\right) \right\}\mathrm{d}x. \end{aligned} \tag{9}$$

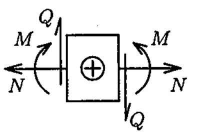

Figure 4: Stress resultant (force) notations

The stress resultants in Equation 9 are defined as:

$$
\begin{aligned}
(N^{u}, M^{u}, Q^{u}) &= \int_{-(l_1+t_1)}^{-l_1} b_1(\sigma_{xx}^{u}, z\,\sigma_{xx}^{u}, \tau_{xz}^{u})\,\mathrm{d}z,\\
(N^{\mathcal{L}}, M^{\mathcal{L}}, Q^{\mathcal{L}}) &= \int_{l_2}^{l_2+t_2} b_2(\sigma_{xx}^{\mathcal{L}}, z\,\sigma_{xx}^{\mathcal{L}}, \tau_{xz}^{\mathcal{L}})\,\mathrm{d}z,\\
(M^{w}, Q^{w}) &= \int_{-l_1}^{l_2} t_0(z\,\sigma_{xx}^{w}, \tau_{xz}^{w})\,\mathrm{d}z. \qquad (10)
\end{aligned}
$$

The stress resultants shown above can be interpreted in the same way as in fundamental beam theory found in elementary strength of materials. The notation is shown in Figure 4 for clarity.

Here, another assumption is made on an identical material properties of upper and lower concrete flanges, i.e. modulus of elasticity, $E_2 = E_1$ and shear modulus of elasticity, $G_2 = G_1$. The stress–strain relations for each element can then be written as shown below (k is shear correction factor):

$$
\begin{aligned}
\sigma_{xx}^{w} &= E_0\varepsilon_{xx}^{w}, & \tau_{xz}^{w} &= G_0\gamma_{xz}^{w},\\
\sigma_{xx}^{u} &= E_1\varepsilon_{xx}^{u}, & \tau_{xz}^{u} &= kG_1\gamma_{xz}^{u},\\
\sigma_{xx}^{\mathcal{L}} &= E_1\varepsilon_{xx}^{\mathcal{L}}, & \tau_{xz}^{\mathcal{L}} &= kG_1\gamma_{xz}^{\mathcal{L}}. \qquad (11)
\end{aligned}
$$

With the above stress–strain relations, one can write the stress resultants in terms of displacements as shown below:

$$
\begin{aligned}
N^{u} &= E_1A_1\left(l_1\frac{\mathrm{d}\alpha}{\mathrm{d}x}+\frac{t_1}{2}\frac{\mathrm{d}\phi}{\mathrm{d}x}\right),\\
N^{\mathcal{L}} &= -E_1A_2\left(l_2\frac{\mathrm{d}\alpha}{\mathrm{d}x}-\frac{t_2}{2}\frac{\mathrm{d}\phi}{\mathrm{d}x}\right),\\
M^{w} &= -E_0t_0\left(\frac{l_1^3}{3}+\frac{l_2^3}{3}\right)\frac{\mathrm{d}\alpha}{\mathrm{d}x},\\
M^{u} &= -E_1A_1l_1\left(l_1+\frac{t_1}{2}\right)\frac{\mathrm{d}\alpha}{\mathrm{d}x}-E_1A_1t_1\left(\frac{l_1}{2}+\frac{t_1}{3}\right)\frac{\mathrm{d}\phi}{\mathrm{d}x},\\
M^{\mathcal{L}} &= -E_1A_2l_2\left(l_2+\frac{t_2}{2}\right)\frac{\mathrm{d}\alpha}{\mathrm{d}x}-E_1A_2t_2\left(\frac{l_2}{2}+\frac{t_2}{3}\right)\frac{\mathrm{d}\phi}{\mathrm{d}x},\\
Q^{w} &= G_0A_0\left(\frac{\mathrm{d}w}{\mathrm{d}x}-\alpha\right),\\
Q^{u} &= kG_1A_1\left(\frac{\mathrm{d}w}{\mathrm{d}x}-\phi\right),\\
Q^{\mathcal{L}} &= kG_1A_2\left(\frac{\mathrm{d}w}{\mathrm{d}x}-\phi\right). \qquad (12)
\end{aligned}
$$

The virtual potential energy of external transverse load, q can be written as:

$$
\delta V = -\int_0^L q\,\delta w\,\mathrm{d}x. \qquad (13)
$$

Finally, substituting Equation 9 and Equation 13 into the following virtual total potential energy function:

$$
\delta\Pi = \delta U + \delta V, \qquad (14)
$$

and applying the principle of virtual displacements, $\delta\Pi = 0$, one can obtained:

Equilibrium equations:

$$
\begin{aligned}
q &= -\frac{\mathrm{d}Q^{w}}{\mathrm{d}x}-\frac{\mathrm{d}Q^{u}}{\mathrm{d}x}-\frac{\mathrm{d}Q^{\mathcal{L}}}{\mathrm{d}x}, & (15)\\
0 &= -\frac{\mathrm{d}M^{w}}{\mathrm{d}x}+l_1\frac{\mathrm{d}N^{u}}{\mathrm{d}x}-l_2\frac{\mathrm{d}N^{\mathcal{L}}}{\mathrm{d}x}+Q^{w}, & (16)\\
0 &= \frac{\mathrm{d}M^{u}}{\mathrm{d}x}+\frac{\mathrm{d}M^{\mathcal{L}}}{\mathrm{d}x}+l_1\frac{\mathrm{d}N^{u}}{\mathrm{d}x}-l_2\frac{\mathrm{d}N^{\mathcal{L}}}{\mathrm{d}x}\\
&\quad -Q^{u}-Q^{\mathcal{L}}, & (17)
\end{aligned}
$$

and *Boundary conditions:*

Natural	Essential	
$Q^{w}+Q^{u}+Q^{\mathcal{L}}$,	w,	(18)
$M^{w}-l_1N^{u}+l_2N^{\mathcal{L}}$,	α,	(19)
$M^{u}+M^{\mathcal{L}}+l_1N^{u}-l_2N^{\mathcal{L}}$,	ϕ.	(20)

Using stress resultant–displacement relations (Equation 12), the equations of equilibrium can be expressed in terms of the displacements as:

$$
\begin{aligned}
q &= -\mathrm{g}_1\left(\frac{\mathrm{d}^2w}{\mathrm{d}x^2}-\frac{\mathrm{d}\phi}{\mathrm{d}x}\right)-\mathrm{g}_0\left(\frac{\mathrm{d}^2w}{\mathrm{d}x^2}-\frac{\mathrm{d}\alpha}{\mathrm{d}x}\right), & (21)\\
0 &= \mathrm{g}_0\left(\frac{\mathrm{d}w}{\mathrm{d}x}-\alpha\right)+\mathrm{e}_0\frac{\mathrm{d}^2\alpha}{\mathrm{d}x^2}+\mathrm{e}_1\frac{\mathrm{d}^2\phi}{\mathrm{d}x^2}, & (22)\\
0 &= \mathrm{g}_1\left(\frac{\mathrm{d}w}{\mathrm{d}x}-\phi\right)+\mathrm{e}_1\frac{\mathrm{d}^2\alpha}{\mathrm{d}x^2}+\mathrm{e}_2\frac{\mathrm{d}^2\phi}{\mathrm{d}x^2}, & (23)
\end{aligned}
$$

where:

$$
\begin{aligned}
\mathrm{g}_0 &= G_0A_0,\\
\mathrm{g}_1 &= kG_1(A_1+A_2),\\
\mathrm{e}_0 &= E_0t_0\left(\frac{l_1^3}{3}+\frac{l_2^3}{3}\right)+E_1\left(A_1l_1^2+A_2l_2^2\right),\\
\mathrm{e}_1 &= \frac{E_1}{2}\left(A_1t_1l_1+A_2t_2l_2\right),\\
\mathrm{e}_2 &= \frac{E_1}{3}\left(A_1t_1^2+A_2t_2^2\right).
\end{aligned}
$$

Equilibrium equations (Equation 21–23) and boundary conditions (Equation 18–20) constitute a system of boundary value problem to be solved.

2.2 Solution of Three–Function Beam Theory

By a well–established systematic method in solving system of differential equations, the homogeneous solution of the equilibrium equation (Equations 21–23) is found to be:

$$w_h = C_0 + C_1 x + C_2 \frac{x^2}{2} + C_3 \frac{x^3}{3} + C_4 \frac{e^{-\beta x}}{\beta} + C_5 \frac{e^{\beta x}}{\beta}, \quad (24)$$

$$\phi_h = C_1 + C_2 x + C_3 \left(x^2 + 2\eta_2\right) + C_4 \theta_1 e^{-\beta x} - C_5 \theta_1 e^{\beta x}, \quad (25)$$

$$\alpha_h = C_1 + C_2 x + C_3 \left(x^2 + 2\eta_3\right) - C_4 \theta_2 e^{-\beta x} + C_5 \theta_2 e^{\beta x}. \quad (26)$$

And a particular solution for a case of uniformly distributed transverse load, q along the beam are:

$$w_p = \frac{q}{\eta_1} \frac{x^4}{24}, \quad (27)$$

$$\phi_p = \frac{q\eta_2}{\eta_1} x + \frac{q}{\eta_1} \frac{x^3}{6}, \quad (28)$$

$$\alpha_p = \frac{q\eta_3}{\eta_1} x + \frac{q}{\eta_1} \frac{x^3}{6}, \quad (29)$$

where:

$$\beta^2 = \frac{\eta_1}{(\mathrm{e}_0 \mathrm{e}_2 - \mathrm{e}_1^2)\eta_4},$$

$$\theta_1 = \frac{\mathrm{g}_0 \eta_3 \eta_4}{\eta_2 - \eta_3}, \qquad \theta_2 = \frac{\mathrm{g}_1 \eta_2 \eta_4}{\eta_2 - \eta_3},$$

$$\eta_1 = \mathrm{e}_0 + 2\mathrm{e}_1 + \mathrm{e}_2, \qquad \eta_2 = \frac{\mathrm{e}_1 + \mathrm{e}_2}{\mathrm{g}_1},$$

$$\eta_3 = \frac{\mathrm{e}_0 + \mathrm{e}_1}{\mathrm{g}_0}, \qquad \eta_4 = \frac{\mathrm{g}_0 + \mathrm{g}_1}{\mathrm{g}_0 \mathrm{g}_1}.$$

Note here that a term $(\mathrm{e}_0 \mathrm{e}_2 - \mathrm{e}_1^2)$ in constant β is positive–definite.

Six unknown constants in the homogeneous solution can be found by considering appropriate boundary conditions at both ends of the beam.

2.3 Two–Function Beam Theory

A three displacement functions based beam model is formulated in section 2.1, and its solution is given in section 2.2. In this section, a beam theory based on two displacement functions deduced from the three displacement functions is presented.

The reduction is made by assuming that the upper and lower flanges can be simply expressed by the Euler–Bernoulli beam theory, while the web still satisfies the Timoshenko beam assumption. The displacement functions for this two–function beam theory can be deduced from Equation 6 by substituting $\hat{\phi} = \mathrm{d}\hat{w}/\mathrm{d}x$, and are shown below:

$$\begin{aligned} \hat{u}^{w} &= -z\hat{\alpha}, \\ \hat{u}^{u} &= l_1 \hat{\alpha} - (z + l_1)\frac{\mathrm{d}\hat{w}}{\mathrm{d}x}, \\ \hat{u}^{\mathcal{L}} &= -l_2 \hat{\alpha} - (z - l_2)\frac{\mathrm{d}\hat{w}}{\mathrm{d}x}, \\ \hat{w}^{w} &= \hat{w}^{u} = \hat{w}^{\mathcal{L}} = \hat{w}. \end{aligned} \quad (30)$$

Small hat over each character designates a quantity belonging to this two–function beam theory.

Stress resultant–displacement relations can be obtained by directly substituting $\hat{\phi} = \mathrm{d}\hat{w}/\mathrm{d}x$ into Equations 12 and are shown here:

$$\begin{aligned} \hat{N}^{u} &= E_1 A_1 \left(l_1 \frac{\mathrm{d}\hat{\alpha}}{\mathrm{d}x} + \frac{t_1}{2} \frac{\mathrm{d}^2 \hat{w}}{\mathrm{d}x^2}\right), \\ \hat{N}^{\mathcal{L}} &= -E_1 A_2 \left(l_2 \frac{\mathrm{d}\hat{\alpha}}{\mathrm{d}x} + \frac{t_2}{2} \frac{\mathrm{d}^2 \hat{w}}{\mathrm{d}x^2}\right), \\ \hat{M}^{w} &= -E_0 t_0 \left(\frac{l_1^3}{3} + \frac{l_2^3}{3}\right) \frac{\mathrm{d}\hat{\alpha}}{\mathrm{d}x}, \\ \hat{M}^{u} &= -E_1 A_1 l_1 \left(l_1 + \frac{t_1}{2}\right) \frac{\mathrm{d}\hat{\alpha}}{\mathrm{d}x} - E_1 A_1 t_1 \left(\frac{l_1}{2} + \frac{t_1}{3}\right) \frac{\mathrm{d}^2 \hat{w}}{\mathrm{d}x^2}, \\ \hat{M}^{\mathcal{L}} &= -E_1 A_2 l_2 \left(l_2 + \frac{t_2}{2}\right) \frac{\mathrm{d}\hat{\alpha}}{\mathrm{d}x} - E_1 A_2 t_2 \left(\frac{l_2}{2} + \frac{t_2}{3}\right) \frac{\mathrm{d}^2 \hat{w}}{\mathrm{d}x^2}, \\ \hat{Q}^{w} &= G_0 A_0 \left(\frac{\mathrm{d}w}{\mathrm{d}x} - \alpha\right). \end{aligned} \quad (31)$$

Shearing force resisted by upper and lower flanges can not be calculated by stress–strain relations because the Euler–Bernoulli beam's assumption provides no transverse shear strain. The shearing force, however, can be deduced from Equation 17 (this is an equilibrium consideration, thus, it should be called *reaction*[16]):

$$\begin{aligned} \hat{Q}^{u} &= \frac{\mathrm{d}\hat{M}^{u}}{\mathrm{d}x} + l_1 \frac{\mathrm{d}\hat{N}^{u}}{\mathrm{d}x} \\ &= -E_1 A_1 t_1 \left(\frac{l_1}{2} \frac{\mathrm{d}^2 \hat{\alpha}}{\mathrm{d}x^2} + \frac{t_1}{3} \frac{\mathrm{d}^3 \hat{w}}{\mathrm{d}x^3}\right), \\ \hat{Q}^{\mathcal{L}} &= \frac{\mathrm{d}\hat{M}^{\mathcal{L}}}{\mathrm{d}x} - l_2 \frac{\mathrm{d}\hat{N}^{\mathcal{L}}}{\mathrm{d}x} \\ &= -E_2 A_2 t_2 \left(\frac{l_2}{2} \frac{\mathrm{d}^2 \hat{\alpha}}{\mathrm{d}x^2} + \frac{t_2}{3} \frac{\mathrm{d}^3 \hat{w}}{\mathrm{d}x^3}\right). \end{aligned} \quad (32)$$

It is noted here that the same form of shearing force $\hat{Q}^{u}$ and $\hat{Q}^{\mathcal{L}}$ can be obtained based on the variational principle if one works on displacement functions in Equation 30 directly.

In a similar study by Kato *et al.* [14], only the last term involving deflection of the girder ($\hat{w}$) seems to be considered.

The first equilibrium equations is deduced by substituting Equation 17 into Equation 15. The second equilibrium equation is in the same form as Equation 16:

$$q = -\frac{\mathrm{d}^2 \hat{M}^{u}}{\mathrm{d}x^2} - l_1 \frac{\mathrm{d}^2 \hat{N}^{u}}{\mathrm{d}x^2} - \frac{\mathrm{d}^2 \hat{M}^{\mathcal{L}}}{\mathrm{d}x^2} + l_2 \frac{\mathrm{d}^2 \hat{N}^{\mathcal{L}}}{\mathrm{d}x^2} - \frac{\mathrm{d}\hat{Q}^{\mathcal{L}}}{\mathrm{d}x}, \quad (33)$$

$$0 = -\frac{\mathrm{d}\hat{M}^{w}}{\mathrm{d}x} + l_1 \frac{\mathrm{d}\hat{N}^{u}}{\mathrm{d}x} - l_2 \frac{\mathrm{d}\hat{N}^{\mathcal{L}}}{\mathrm{d}x} + \hat{Q}^{w}, \quad (34)$$

with boundary conditions:

Natural	Essential	
$\hat{Q}^w + \hat{Q}^u + \hat{Q}^{\mathcal{L}},$	$\hat{w},$	(35)
$\hat{M}^w - l_1\hat{N}^u + l_2\hat{N}^{\mathcal{L}},$	$\hat{\alpha},$	(36)
$\hat{M}^u + \hat{M}^{\mathcal{L}} + l_1\hat{N}^u - l_2\hat{N}^{\mathcal{L}},$	$\frac{\mathrm{d}\hat{w}}{\mathrm{d}x}.$	(37)

Substituting stress resultant–displacement relations (Equation 31 and 32) into Equation 33 and 34 yields the equilibrium equations in terms of the displacements as:

$$q = \hat{\mathrm{e}}_2\frac{\mathrm{d}^4\hat{w}}{\mathrm{d}x^4} + \hat{\mathrm{e}}_1\frac{\mathrm{d}^3\hat{\alpha}}{\mathrm{d}x^3} - \hat{\mathrm{g}}_0\left(\frac{\mathrm{d}^2\hat{w}}{\mathrm{d}x^2} - \frac{\mathrm{d}\hat{\alpha}}{\mathrm{d}x}\right), \tag{38}$$

$$0 = \hat{\mathrm{g}}_0\left(\frac{\mathrm{d}\hat{w}}{\mathrm{d}x} - \hat{\alpha}\right) + \hat{\mathrm{e}}_0\frac{\mathrm{d}^2\hat{\alpha}}{\mathrm{d}x^2} + \hat{\mathrm{e}}_1\frac{\mathrm{d}^3\hat{w}}{\mathrm{d}x^3}, \tag{39}$$

where:

$$\hat{\mathrm{g}}_0 = G_0A_0,$$

$$\hat{\mathrm{e}}_0 = E_0t_0\left(\frac{l_1^3}{3} + \frac{l_2^3}{3}\right) + E_1\left(A_1l_1^2 + A_2l_2^2\right),$$

$$\hat{\mathrm{e}}_1 = \frac{E_1}{2}\left(A_1t_1l_1 + A_2t_2l_2\right),$$

$$\hat{\mathrm{e}}_2 = \frac{E_1}{3}\left(A_1t_1^2 + A_2t_2^2\right).$$

2.4 Solution of Two–Function Beam Theory

Similar to section 2.2, one can obtain the homogeneous solution of the equilibrium equations (Equation 38, 39) as shown below:

$$\hat{w}_h = \hat{C}_0 + \hat{C}_1x + \hat{C}_2\frac{x^2}{2} + \hat{C}_3\frac{x^3}{3} + \hat{C}_4\frac{e^{-\hat{\beta}x}}{\hat{\beta}} + \hat{C}_5\frac{e^{\hat{\beta}x}}{\hat{\beta}}, \tag{40}$$

$$\hat{\alpha}_h = \hat{C}_1 + \hat{C}_2x + \hat{C}_3\left(x^2 + 2\hat{\eta}_2\right) + \hat{C}_4\hat{\theta}_1e^{-\hat{\beta}x} - \hat{C}_5\hat{\theta}_1e^{\hat{\beta}x}. \tag{41}$$

and a particular solution for a case of uniformly distributed transverse load, q along the beam as:

$$\hat{w}_p = \frac{q}{\hat{\eta}_1}\frac{x^4}{24}, \tag{42}$$

$$\hat{\alpha}_p = \frac{q\hat{\eta}_2}{\hat{\eta}_1}x + \frac{q}{\hat{\eta}_1}\frac{x^3}{6}. \tag{43}$$

where:

$$\hat{\beta}^2 = \frac{\hat{\eta}_1\hat{\mathrm{g}}_0}{(\hat{\mathrm{e}}_0\hat{\mathrm{e}}_2 - \hat{\mathrm{e}}_1^2)}, \quad \hat{\theta}_1 = \frac{\hat{\mathrm{e}}_1 + \hat{\mathrm{e}}_2}{\hat{\mathrm{e}}_0 + \hat{\mathrm{e}}_1},$$

$$\hat{\eta}_1 = \hat{\mathrm{e}}_0 + 2\hat{\mathrm{e}}_1 + \hat{\mathrm{e}}_2, \quad \hat{\eta}_2 = \frac{\hat{\mathrm{e}}_0 + \hat{\mathrm{e}}_1}{\hat{\mathrm{g}}_0}.$$

This completes the derivation of three–function and two–function beam theory.

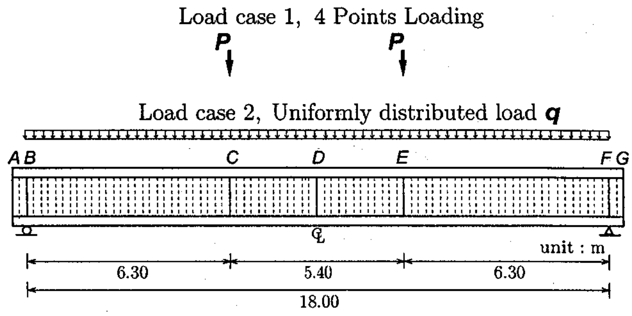

Figure 5: Representative girder

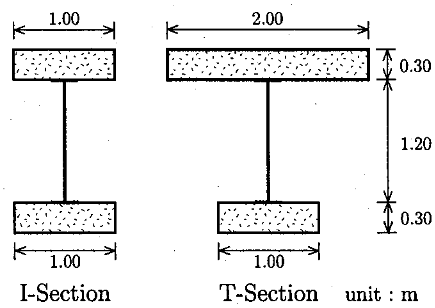

Figure 6: I and T section

It is noted here that it is possible to derive a four–function beam theory by working on assumed displacement functions in Equation 3 directly. But it is found that its equilibrium equations are complex and leads to a solution involving 8 different exponential functions (comparing to 2, in Equation 24 and 40). So in this study, up to three–function beam model is derived and studied.

For upper and lower flanges in three–function beam theory, a more refined beam theory which does not require a shear correction factor can be used instead of Timoshenko beam theory [19) 21)]. The refined theory is a third–order one which completely satisfies free surface stress condition requirement. And it also requires higher–order stress resultant–displacement relation. This seems to complicate the development and hinders an interpretation of the equilibrium equations and boundary conditions.

3. Application to Corrugated Steel Web Girder

In this section, the developed theories are applied to solve for shearing force in web of a number of girder. The problem is also solved by the finite element analysis.

3.1 I–, T– and Box Girder

Figure 5 shows a simply supported PC girder with corrugated steel web to be analyzed in this section. Three typical sections as shown in Figure 6 and Figure 7 for I–, T– and Box girders are selected as representatives of commonly used girders.

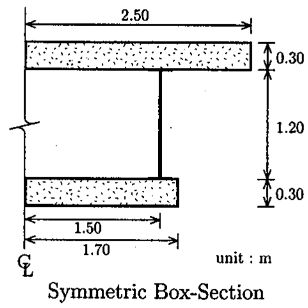

Figure 7: Box section

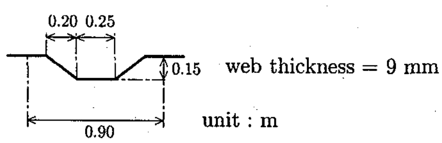

Figure 8: Corrugated web geometry

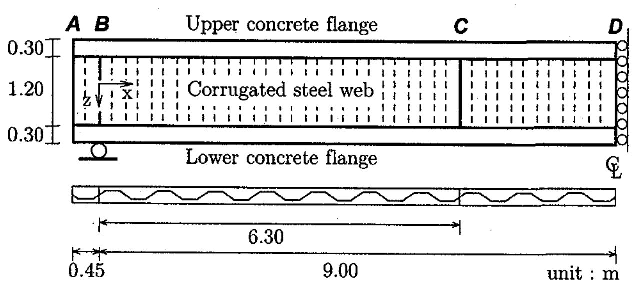

Figure 9: Symmetric half of a simply supported girder

Upper and lower flanges in the girder are assumed poured with concrete of ultimate strength $4.0 \times 10^7\,\mathrm{N/m^2}$ and modulus of elasticity of $3.10 \times 10^{10}\,\mathrm{N/m^2}$, corrugated steel web is SM490Y with modulus of elasticity of $2.0 \times 10^{11}\,\mathrm{N/m^2}$. Calculated shear modulus of elasticity of the concrete and the web are $1.292 \times 10^{10}\,\mathrm{N/m^2}$ and $7.692 \times 10^{10}\,\mathrm{N/m^2}$, respectively (see Equation 57). The corrugated web is made of a 9 mm–thick steel sheet folded into a trapezoidal shape with a dimension as shown in Figure 8. The web is also provided with upper and lower steel flanges and 7 vertical steel stiffeners of the same thickness at location A–G as shown in Figure 5. They are all with 25 cm width.

Symmetry of the girder with respect to its midspan is benefited by requiring only half of a girder to be analyzed. The symmetric half is shown in Figure 9 with detailed dimensions.

The girders are assumed to be loaded by two different load cases as shown in Figure 5. Load case 1 is concentrated 4 points loading, and load case 2 is uniformly distributed load along its clear span.

Effective prestressing force is assumed to cause approximately zero stress and 40% of concrete's ultimate strength stress in upper and lower flanges, respectively. Magnitudes of the load in each case are then calculated to approximately neutralize lower flange's stress. Summary of force parameters is shown in Table 1

Table 1: Prestressing force and load case

Force elements	Section		
	I	T	Box
Prestress force [MN]			
1) Upper flange	0.315	0.72	0.90
2) Lower flange	4.50	4.50	7.65
Load case 1, P [MN]	1.00	1.05	1.70
Load case 2, q [MN/m]	0.16	0.16	0.27

3.2 Theoretical Analysis

Analytical solution can be obtained in an exact manner as when one dues with a deflection problem of loaded beam. The general solution and particular solution given in Section 2.2 and Section 2.4 for three–function (Equation 24–26 and 27–29) and two–function beam theory (Equation 40–41 and 42–43) are already at hand and adequate to solve the problem with both loading cases. The remaining is to evaluate constants of integration from appropriate boundary conditions for each span and each loading case. There is no difference in I–, T– and Box–girder in considering the boundary conditions.

For loading case 1 (4–point load), the symmetric left half of the girder is divided into 3 segments composed of segment A–B, B–C and C–D (refer to Figure 9). The appropriate boundary condition for each point is discussed below (refer to Equation 18–20 and Equation 35–37). The treatment is done for three–function beam theory only because the corresponding boundary conditions for the two–function theory can be deduced directly by substitution, $\hat{\phi} = \mathrm{d}\hat{w}/\,\mathrm{d}x$.

1. *Point A, free end with and without prestressing force*, it requires that:

$$\alpha = \phi, \tag{44}$$

$$Q^w + Q^u + Q^{\mathcal{L}} = 0, \tag{45}$$

to satisfy plane remains plane condition. Bending moment arises from prestressing force is balanced by setting:

$$M^w + M^u + M^{\mathcal{L}} = M_p, \tag{46}$$

where M_p stands for prestressing moment (which is generally negative) and it is zero in a case of no prestressing. Prestressing compressive force is treated separately by the superposition principle.

2. *Point B, interior support*, it requires that:

$$\overset{-}{w} = \overset{+}{w} = 0, \tag{47}$$

$$\overset{-}{\phi} = \overset{+}{\phi}, \tag{48}$$

$$\overset{-}{\alpha} = \overset{+}{\alpha}, \tag{49}$$

$$\bar{M}^{w} - \bar{l}_1\bar{N}^{u} + \bar{l}_2\bar{N}^{\mathcal{L}} = \overset{+}{M}{}^{w} - \overset{+}{l}_1\overset{+}{N}{}^{u} + \overset{+}{l}_2\overset{+}{N}{}^{\mathcal{L}}, \quad (50)$$

$$\bar{M}^{u} + \bar{M}^{\mathcal{L}} + \bar{l}_1\bar{N}^{u} - \bar{l}_2\bar{N}^{\mathcal{L}} = \overset{+}{M}{}^{u} + \overset{+}{M}{}^{\mathcal{L}} + \overset{+}{l}_1\overset{+}{N}{}^{u} - \overset{+}{l}_2\overset{+}{N}{}^{\mathcal{L}}, \quad (51)$$

where − and + signs designated quantities of left and right span, respectively.

3. *Point C, interior connection with applied external force*, this condition is similar to the case of interior support, i.e. Equation 48, 49, 50 and 51 are valid. Additional requirements are:

$$\bar{w} = \overset{+}{w}, \quad (52)$$

$$(\bar{Q}^{w} + \bar{Q}^{u} + \bar{Q}^{\mathcal{L}}) - (\overset{+}{Q}{}^{w} + \overset{+}{Q}{}^{u} + \overset{+}{Q}{}^{\mathcal{L}}) = P, \quad (53)$$

here, P is an applied external force.

4. *Point D, symmetric midspan*, no rotation is allowed:

$$\alpha = 0, \quad (54)$$

$$\phi = 0, \quad (55)$$

and it requires vanishing of shearing force:

$$Q^{w} + Q^{u} + Q^{\mathcal{L}} = 0. \quad (56)$$

For loading case 2 (uniformly distributed load), the girder is divided into 2 segments, A–B and B–D and the boundary conditions are that of case 1, case 2 and case 4 above.

Other quantities for the solution of the differential equations are materials properties which are of very important. Shear modulus of elasticity of concrete, G_1 is postulated to be derivable by a relation:

$$G = \frac{E}{2(1+\nu)}, \quad (57)$$

with the Poisson's ratio of 0.2.

Shear modulus of elasticity of corrugated steel web, G_0 is derived by the same relation ($\nu = 0.3$). A reduced modulus of elasticity of the web, E_0 however, is set as zero in this study. A reader who is interested in equivalent orthotropic properties of corrugated sheet is referred to a work of Briassoulis[22] for a wealth information on the topic of a curved corrugated sheet. For reduced modulus of elasticity in extension for trapezoidal corrugated sheet, one may find a work of Tapankeaw *et al.*[23] and that of Johnson and Cafolla[24] helpful.

3.3 Classical Theories

For comparison purpose, calculation results based on the classical Euler–Bernoulli beam theory and the classical Timoshenko beam theory are also examined.

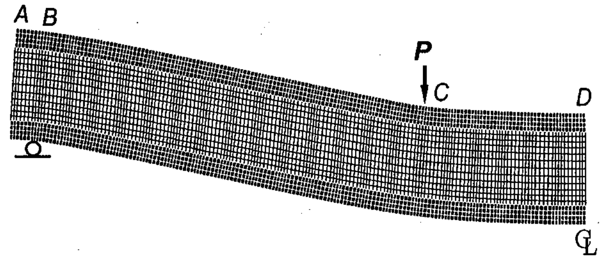

Figure 10: Magnified deformed I–girder under load case 1 (Flanges are in inverted color)

Shear deformation is not considered in the Euler–Bernoulli theory but the Timoshenko theory does. In this calculation, shearing force in the Timoshenko theory is assumed to be resisted entirely by the web (with shear correction factor 1.0) while bending force to be resisted by upper and lower flanges.

3.4 Finite Element Analysis

A numerical calculation by the finite element analysis is also carried out in this study. The girder is modelled and analyzed in a generous finite element analysis program, ABAQUS. Concrete flanges are discretized into matrices of three-dimensional 8–node linear brick element, C4D8. Corrugated steel web, steel flanges and stiffeners are assembled from 4–node linear shell element, S4 (An example of the finite element model is shown in Figure 10).

A condition of plane remains plane at the end of the girder is achieved by utilizing rigid element. Load is directly placed on a small area (or small band) on the upper flange over corrugated web and linear analysis is carried out in this study.

3.5 Analysis Discussions

Figure 10 shows a magnified deformation of I–girder under load case 1. Unparalleled deformed section of concrete flanges and corrugated web can be noticed in the figure and this confirms the assumption on different rotation of the elements.

Shearing forces in corrugated web calculated by the finite element analysis and those predicted by developed beam theories are shown in Figure 11 to Figure 14. The cases of T– and Box girder for load case 2 are omitted here to save space. A very good agreement on the calculated shearing force is found in all figures. Both three– and two–function beam theory yield predicted shear forces almost the same and they are very close to those calculated by the finite element analysis.

Vertical deformations of the girder are shown in Figure 15 to Figure 17, for I–, T– and Box girder under load case 1. The results from finite element analysis refer to a line connecting centroid of the lower flanges and those marked with 'FEA w/o shear lag' are obtained from the model with additional lateral restraint on the upper and lower flanges not to allow for shear lag in them.

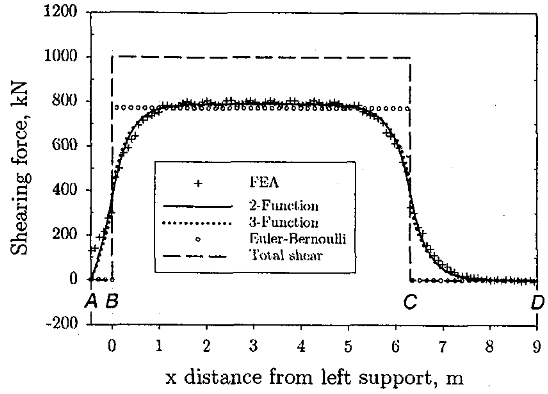

Figure 11: Shearing force in web of I–girder under load case 1

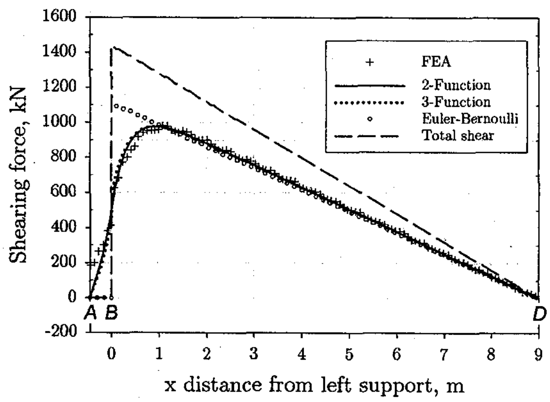

Figure 12: Shearing force in web of I–girder under load case 2

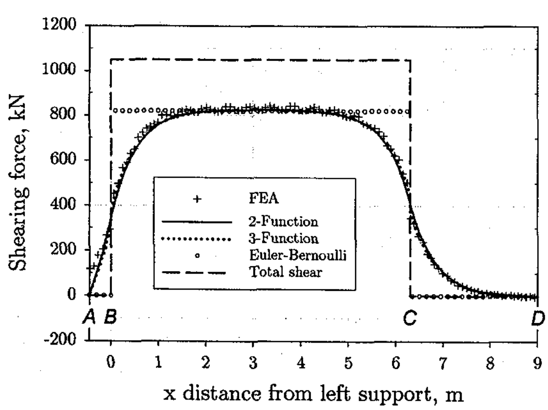

Figure 13: Shearing force in web of T–girder under load case 1

From the figures, it is found that the vertical deformation of the girders predicted by the developed theory are almost the same as those calculated by the finite element analysis. Especially, they are in very good agreement with results by the finite element analysis for no shear lag case, as the phenomenon is not considered in this study. On the other hand, the results based on the Euler–Bernoulli beam theory and Timoshenko beam theory evidently give erroneous predictions.

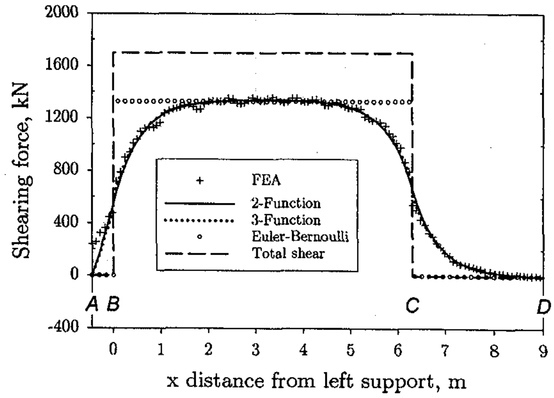

Figure 14: Shearing force in web of Box girder under load case 1

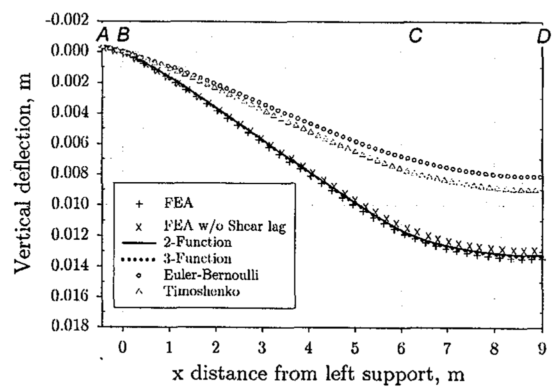

Figure 15: Vertical displacement of I–girder under load case 1

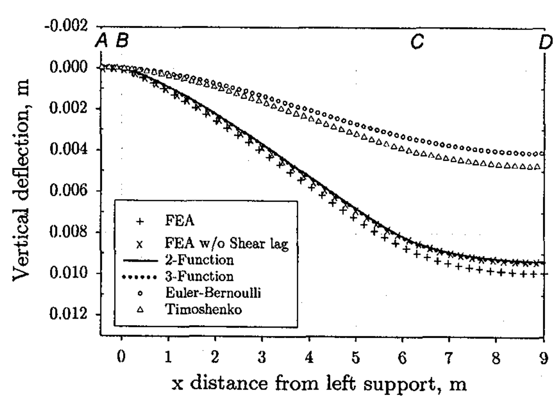

Figure 16: Vertical displacement of T–girder under load case 1

4. Conclusions

The extended elastic shear deformable beam theory is developed in this study. The equations of equilibrium and their associated boundary conditions are derived by the principle of virtual displacement. Theory based on three and two displacement functions are obtained and they are verified with a calculation comparing with the finite element analysis. A good agreement on the shearing force distribution in corrugated web is

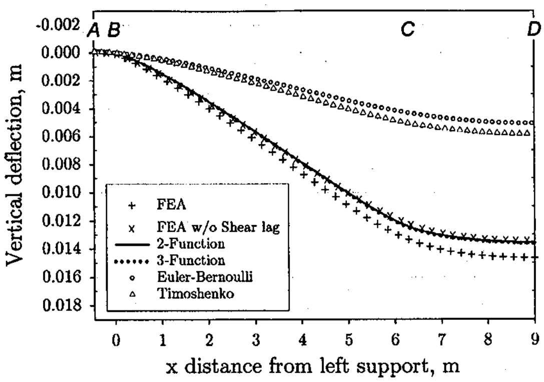

Figure 17: Vertical displacement of Box girder under load case 1

found.

In conclusion, the developed theory is accurate enough to be applied for prediction of force and deflection in PC girder with corrugated steel web.

References

1) Johnson, R. P. and Cafolla, J., Local Flange Buckling in Plate Girders with Corrugated Webs, *Proceedings of the Institution of Civil Engineers. Structures and buildings*, Vol. 123(May), pp. 148–156, 1997.

2) Combault, J. (Ohura, T. translator), The Maupre Viaduct near Charolees, France, *Journal of Japan Pre stressed Concrete Engineering Association*, Vol. 34(1), pp. 63–71, 1992. (in Japanese)

3) Takahashi, I., Uchida, M., Matsumoto, M. and Konishi, T., Design and Construction Reports of the PC Bridges with Corrugated Steel Webs, *Kawada Technical Report*, Japan, Tokyo, Vol. 21(Jan), pp. 82–85, 2002. (in Japanese)

4) Research Group of Composite Structures with Corrugated Steel Web, *Design manual of PC box girders with corrugated steel webs (Draft)*, Japan, Tokyo, 1998. (in Japanese)

5) Johnson, R. P. and Cafolla, J., Corrugated Webs in Plate Girders for Bridges, *Proceedings of the Institution of Civil Engineers. Structures and buildings*, Vol. 123(May), pp. 157–164, 1997.

6) Mo, Y. L., Jeng, C. and Chang Y. S., Torsional Behavior of Prestressed Concrete Box-Girder Bridges with Corrugated Steel Webs, *ACI Structural Journal*, Vol. 97(6), pp. 849–859, 2000.

7) Watanabe, E., Kadotani, T., Kano, E., Utsunomiya, T. and Machimdamrong, C., Corrugated Steel Webs in Prestress Girders, *Proceeding of the Fourth U.S.–Japan Seminar: Advanced Stability Seismicity Concept for Performance–based Design of Steel and Composite Structures*, Japan, Kyoto, July 23–26, 2001.

8) Yamaguchi, K., Yamaguchi, T. and Ikeda, S., The Mechanical Behavior of Composite Prestressed Concrete Girders with Corrugated Steel Webs, *Concrete Library*, JSCE, No. 31, pp. 183–209, 1998.

9) Elgaaly, M., Hamilton, R. W. and Seshadri, A., Shear Strength of Beams with Corrugated Webs, *Journal of Structural Engineering*, ASCE, Vol. 122(4), pp. 390–398, 1996.

10) Elgaaly, M., Seshadri, A. and Hamilton, W., Bending Strength of Steel Beams with Corrugated Webs, *Journal of Structural Engineering*, ASCE, Vol. 123(6), pp. 772–782, 1997.

11) Oehlers, D. J. and Bradford, M. A., *Composite Steel and Concrete Structural Members: Fundamental Behavior*, Elsevier, Oxford, 1995.

12) Taniguchi, N. and Yoda, T., Study on a Simple Method for Bending Analysis of Composite Girders with Corrugated Steel Webs, *Journal of Structural Mechanics and Earthquake Engineering*, JSCE, No. 577(I–41), pp. 107–120, 1997. (in Japanese)

13) Shirozu, A., Sano, Y. and Oshita, S., A Study on a Analytical Method using "The Constant Shear Flow Panels" for Composite Bridges with Corrugated Steel Webs, *Journal of Structural Engineering*, JSCE, Vol. 46A, pp. 1667–1674, 2000. (in Japanese)

14) Kato, H., Kawabata A. and Nishimura, N., Practical Calculation Formula on Displacements and Stress Resultants of Steel-Concrete Mixed Girders with Corrugated Steel Web, *Journal of Structural Mechanics and Earthquake Engineering*, JSCE, No. 703(I–59), pp. 293–300, 2002. (in Japanese)

15) Reddy, J. N., A Simple Higher–Order Theory for Laminated Composite Plates, *Journal of Applied Mechanics*, Vol. 51(Dec), ASME, pp. 745–752, 1984.

16) Chen, W. F. and Atsuta, T., *Theory of Beam–Columns, Volume 1: In-Plane Behavior and Design*, McGraw-Hill, 1976.

17) Hussain, M. I. and Libove, C., Stiffness Tests of Trapezoidally Corrugated Shear Webs, *Journal of the Structural Division*, ASCE, Vol. 103 (ST5), pp. 971–987, 1977.

18) Timoshenko, S. P., On the Correction for Shear of the Differential Equation for Transverse Vibrations of Prismatic Bars, *Philosophical Magazine*, Ser. 6, Vol. 41, pp. 744–746, 1921.

19) Wang, C. M., Reddy, J. N. and Lee, K. H., *Shear Deformable Beams and Plates: Relationships with Classical Solutions*, Elsevier Science, 2000.

20) Reddy, J. N., *Energy and Variational Methods in Applied Mechanics, With an Introduction to the Finite Element Method*, John Wiley & Sons, 1984.

21) Levinson, M., A new rectangular beam theory, *Journal of Sound and Vibration*, 74(1), pp. 81–87, 1981.

22) Briassoulis, D., Equivalent Orthotropic Properties of Corrugated Sheets, *Computers and Structures*, Vol. 23(2), pp. 129–138, 1986.

23) Tapankeaw, N., Huang, L. and Hikosaka, H., Nonlinear Analysis of Prestressed Concrete Beam with Corrugated Steel Web, *Proceeding of the Fourth International Summer Symposium*, Japan, Kyoto, August 3, 2002, pp. 43–46.

24) Johnson, R. P. and Cafolla, J., Fabrication of steel bridge girders with corrugated webs, *The Structural Engineer*, Vol. 75(8), pp. 133–135, 1997.

(Received September 13,2002)